Solid-State Electronics 54 (2010) 488–491

Contents lists available at ScienceDirect

Solid-State Electronics

journal homepage: www.elsevier.com/locate/sse

AlInGaN ultraviolet-C photodetectors with a Ni/Ir/Au multilayer metal contact

Han Cheng Lee [a], Yan Kuin Su [a,c,*], Jia Ching Lin [b], Yi Cheng Cheng [b], Ta Ching Li [b], Kuo Jen Chang [b]

[a] Advanced Optoelectronic Technology Center, Institute of Microelectronics, Department of Electrical Engineering, National Cheng Kung University, Tainan 701, Taiwan
[b] Materials and Electro-Optics Research Division, Chung Shan Institute of Science and Technology, Taoyuan 325, Taiwan
[c] Department of Electrical Engineering, Kun Shan University, Yongkang City, Tainan 710, Taiwan

ARTICLE INFO

Article history:
Received 23 July 2009
Received in revised form 24 November 2009
Accepted 1 December 2009
Available online 15 January 2010

The review of this paper was arranged by Prof. E. Calleja

Keywords:
AlInGaN
Metal–insulator–semiconductor (MIS)
Ultraviolet (UV)
Photodetectors (PDs)

ABSTRACT

Aluminum indium gallium nitride (AlInGaN) metal–insulator–semiconductor (MIS) ultraviolet-C (UV-C) photodetectors (PDs) with a Ni/Ir/Au multilayer contact were proposed and fabricated. The inserting layer of the high work function metal (Ir) can significantly reduce the dark current of PDs and enhance the device performance, which can be attributed to the formation of IrO_2 in multilayer contact. With a 3.5 V reverse bias, it was found that the dark current densities of PDs with a Ni/Au conventional contact and a Ni/Ir/Au multilayer contact were 3.7×10^{-8} A/cm^2 and 8.3×10^{-9} A/cm^2, respectively. Although the responsivities of these two different PDs are almost the same, the rejection ratio of AlInGaN MIS PD with a Ni/Ir/Au contact was larger than that of PD with a Ni/Au contact.

1. Introduction

Gallium nitride-based semiconductor devices have been developed for 20 years. III–V nitride semiconductors have attracted a lot of attention for light emitting devices (LEDs) [1], laser diodes (LDs) [2], photodetectors [3,4], and high-power high-frequency transistors [5,6]. For ultraviolet (UV) range detecting applications, the nitride-based materials are the best candidates used in various commercial and military applications such as space communications, missile detection, UV astronomy, ozone-layer monitoring, and fire alarms. The visible-blind PDs can be simply fabricated by binary GaN materials, due to its absorption edge of 360 nm. The solar-blind PDs, however, usually use ternary AlGaN materials to shorten their cut-off wavelengths below 280 nm [7–9]. Unfortunately, the surface cracks are generally observed in AlGaN/GaN heterostructure, especially on the case with high-Al-content AlGaN layer [10,11]. To solve this issue, one solution is using the lattice-matched (or near-matched) quaternary AlInGaN materials to achieve crack-free structures. In addition, the AlInGaN material has also received attention as a material for optoelectronic devices operating in the UV region [12]. In this paper, an AlInGaN/GaN heterostructure with a crack-free AlInGaN epitaxial layer was realized to fabricate a metal–insulator–semiconductor PDs in UV-C (wavelength < 280 nm) detecting range. For MIS PDs, high quality Schottky contact is a major factor to achieve high device performance. A good Schottky contact will induce a large barrier height which can lead to better device characteristics such as small leakage current and high breakdown voltage. In GaN-based material systems, different high work function metals have been used to form high quality Schottky contacts, such as Pt (5.65 eV) [13], Ni (5.15 eV) [14], Au (5.1 eV) [15] and Ir (5.46 eV) [16–18]. In this study, for obtaining the lower leakage current and better performance of PDs, the Ni/Ir/Au multilayer contact was utilized in PDs. This is due to the IrO_2 can be formed in the Ni/Ir/Au multilayer contact to improve performance of PDs. The properties of AlInGaN MIS PDs with a Ni/Ir/Au multilayer contact was discussed in detail, and the secondary ion mass spectroscopy (SIMS) was used to further investigate the interfacial reaction between the contact and epitaxial layers. The electron spectroscopy for chemical analysis (ESCA) was used to verify the formation of IrO_2.

2. Experimental

AlInGaN/GaN heterostructure samples were all grown on c-face (0 0 0 1) sapphire substrates using a horizontal low-pressure metalorganic chemical vapor deposition (MOCVD) system. Trimethylgallium (TMGa), Trimethylindium (TMIn), Trimethylaluminum (TMAl) and Ammonia (NH_3) were employed as gallium, indium,

* Corresponding author. Address: Advanced Optoelectronic Technology Center, Institute of Microelectronics and Department of Electrical Engineering, National Cheng Kung University, Tainan 701, Taiwan. Tel.: +886 6 275 7575x62382; fax: +886 6 235 6226.
E-mail address: yksu@mail.ncku.edu.tw (Y.K. Su).

0038-1101/$ - see front matter © 2009 Elsevier Ltd. All rights reserved.
doi:10.1016/j.sse.2009.12.022

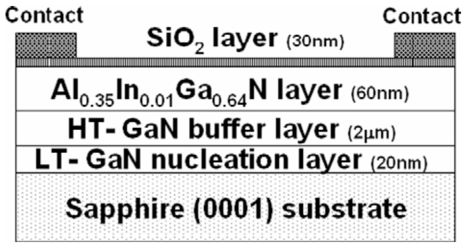

Fig. 1. Schematic structure of AlInGaN MIS UV-C PDs.

aluminum and nitrogen sources, respectively. The device structures of the AlInGaN UV-C PDs consist of a 20 nm-thick GaN nucleation layer grown at 540 °C, a 2 μm-thick undoped GaN buffer layer grown at 1090 °C, and a 60 nm-thick AlInGaN active layer grown at 900 °C. The growth pressures of the u-GaN and AlInGaN layer were 200 and 150 mbar, respectively. The V/III ratios were 8785 and 3789 in the AlInGaN and GaN layer, respectively. The In and Al mole fractions of the AlInGaN active layer were 1% and 35%, respectively, as determined by secondary ion mass spectrometry measurements. By theory calculation, the bandgap of $Al_{0.35}In_{0.01}Ga_{0.64}N$ is around 280 nm [19,20]. X-ray diffraction was also carried out to figure the crystalline qualities of GaN and AlInGaN layers. According to X-ray diffraction analysis, the full width at half-maximum (FWHM) values of the GaN and AlInGaN related peak were 160 and 230 arcsec, respectively. For the purpose of the low dark current characteristics, we first deposited a 30 nm-thick SiO_2 insulating layer on the surface of the AlInGaN/GaN heterostrucutre samples using plasma enhanced chemical vapor deposition [21,22]. After the SiO_2 deposition, the Ni(10 nm)/Au(30 nm) conventional contact, and Ni(10 nm)/Ir(30 nm)/Au(30 nm) multilayer contact were then deposited on the surface of SiO_2 insulating layer by electron beam evaporation. The effective absorption area of all fabricated AlInGaN MIS PDs is 3×10^{-3} cm^2. Fig. 1 shows the schematic structure of AlInGaN MIS PDs used in this study. An HP-4155 semiconductor parameter analyzer was then used to measure the current–voltage (I–V) characteristics of the fabricated devices, and the secondary ion mass spectroscopy was used to examine metal indiffusion between contact metals and AlInGaN epitaxial layers. In order to verify existence of IrO_2, the chemical binding state of IrO_2 at Ir metal layer was investigated by electron spectroscopy for chemical analysis. For photocurrent and spectral responsivity measurements, a xenon-arc lamp was used as the light source. To determine the device's spectral responsivity, one must know the power reaching the device at each wavelength and the current produced by the device at each of those wavelengths. In this system, the power is measured with a calibrated photodiode. Therefore, the spectral responsivity can be calculated by using the current-to-power ratio (A/W).

3. Results and discussion

Fig. 2 shows the dark current density–voltage (J–V) characteristics of these fabricated AlInGaN MIS UV-C PDs measured at room temperature. It can be clearly seen that the dark current of PDs with a Ni/Ir/Au multilayer contact was lower than that of PDs with a Ni/Au conventional contact. With a 3.5 V reverse bias, it was found that the dark current densities of PDs with a Ni/Au contact and a Ni/Ir/Au contact were 3.7×10^{-8} A/cm^2 and 8.3×10^{-9} A/cm^2, respectively. The smaller dark current density observed for PDs with a Ni/Ir/Au contact can be attributed to the fact that this multilayer contact can effectively suppress dark current due to the formation of IrO_2. For further investigating the interfacial reaction between the Ni/Au (Ni/Ir/Au) multilayer contact and AlInGaN epitaxial layers, SIMS measurements were carried out and the results are showed in Figs. 3 and 4. Figs. 3 and 4 show the SIMS depth profiles of AlInGaN MIS PDs with a Ni/Au contact and a Ni/Ir/Au contact, respectively. Obviously, the O atoms were higher than other atoms in Figs. 3a and 4a. This is due to the contribution of SiO_2 layer. The metal oxide could be easily produced at high O atoms. In addition, it was found that the interface was clear between metal contact and AlInGaN epitaxial layers, as shown in Figs. 3b and 4b. From Fig. 3a, the indiffusion phenomenon of Au metal toward the SiO_2 and AlInGaN layer can be clearly observed. In contrast, such indiffusion of Au metal is suppressed by using a Ni/Ir/Au contact, as shown in Fig. 4a. The Ir metal shows the superior Au blocking ability may due to the formation of IrO_2 alloy [23]. Iridium oxide (IrO_x) has advantages of low resistivity (~50 μΩ cm), a high work function (>5 eV), excellent thermal stability, high transmittance to UV light, and high Schottky barrier height (SBH) [24,25]. The IrO_2 then can induce a large barrier height to form a good Schottky contact. Thus, the PDs with a Ni/Ir/Au multilayer contact should have lower leakage current comparing to the PDs with a Ni/Au contact. In order to verify existence of IrO_2 in Ir metal layer, the electron spectroscopy chemical analysis was used to utilize. Fig. 5 shows the Ir4f core level spectra for IrO_2. Two peaks were originated from Ir4$f_{7/2}$ and Ir4$f_{5/2}$. The binding energy of Ir4$f_{7/2}$ and

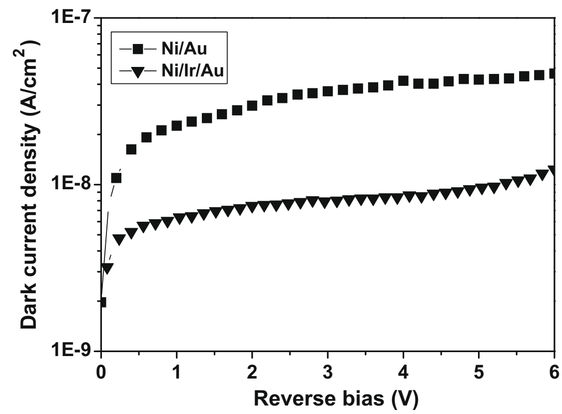

Fig. 2. Dark current density–voltage (J–V) characteristics of PDs with a Ni/Au contact and a Ni/Ir/Au contact.

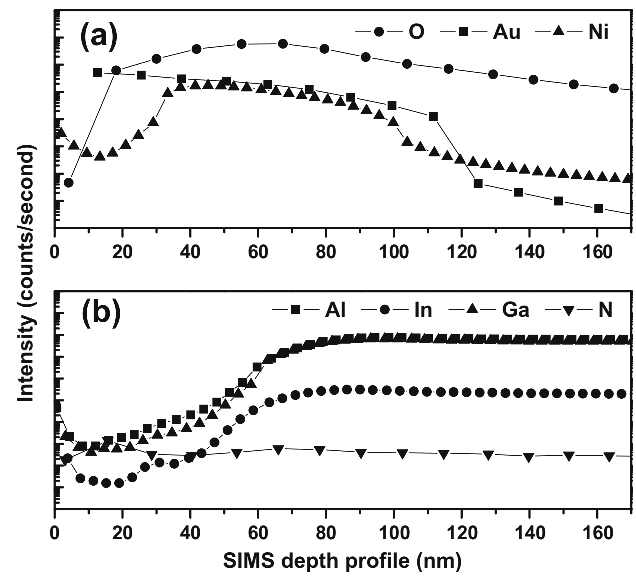

Fig. 3. SIMS depth profiles of the Ni/Au conventional contact on AlInGaN PDs: (a) metal contact (including O atoms) and (b) AlInGaN epitaxial layers.

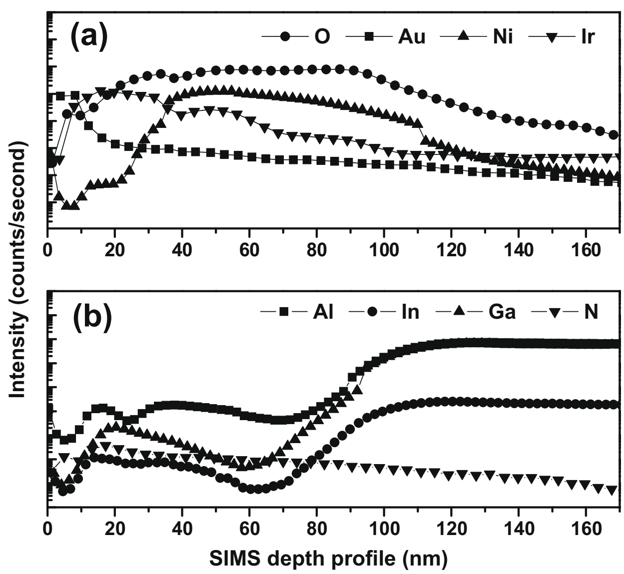

Fig. 4. SIMS depth profiles of the Ni/Ir/Au multilayer contact on AlInGaN PDs: (a) metal contact (including O atoms) and (b) AlInGaN epitaxial layers.

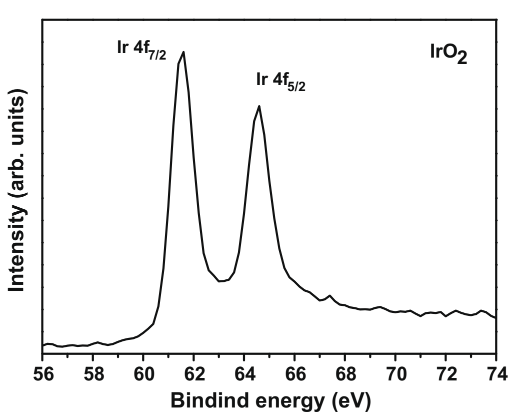

Fig. 5. The ESCA spectra of Ir4*f* core level for IrO_2.

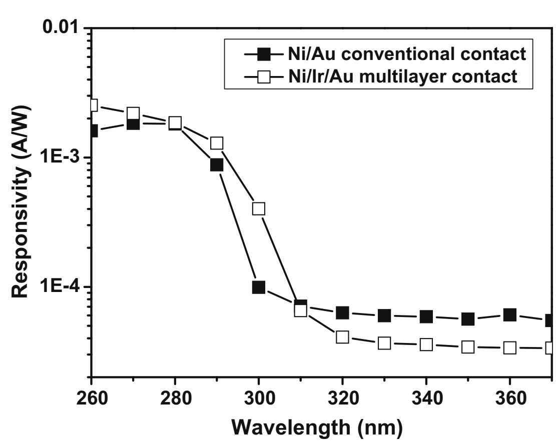

Fig. 6. Spectral responsivity of AlInGaN UV-C PDs with a Ni/Au contact and a Ni/Ir/Au contact under a reverse bias of 3.5 V.

Ir4$f_{5/2}$ were 61.6 and 64.6 eV, respectively, which agrees with the value for IrO_2 [26–28]. These results indicate that IrO_2 were formed at Ir metal layer. The spectral responsivity of AlInGaN UV-C PDs with a Ni/Au conventional contact and a Ni/Ir/Au multilayer contact under a reverse bias of 3.5 V are shown in Fig. 6. It can be clearly seen that the maximum responsivity occurred at around 280 nm, which corresponds to the AlInGaN absorption bandgap. The responsivities of PDs with a Ni/Au contact and a Ni/Ir/Au contact under a reverse bias of 3.5 V were 1.82 mA/W and 1.86 mA/W, respectively. It was also found that the responsivity of PDs with a Ni/Ir/Au contact was lower between 320 nm and 370 nm. Here, we define the rejection ratio as the responsivity measured at 260 nm divided by the responsivity measured at 350 nm. It was found that the rejection ratios of the PDs with a Ni/Ir/Au contact and a Ni/Au contact were 74 and 28.6, under a reverse bias of 3.5 V, respectively. The value of rejection ratio in PDs with a Ni/Ir/Au multilayer contact was large than that of PDs with a Ni/Au contact.

4. Conclusions

AlInGaN MIS UV-C PDs with a Ni/Ir/Au multilayer contact were proposed and fabricated. The inserting layer of the high work function metal (Ir) can significantly reduce the dark current of PDs and enhance the device performance, which can be attributed to the formation of IrO_2 in multilayer contact. With a 3.5 V reverse bias, it was found that the dark current densities of PDs with a Ni/Au contact and a Ni/Ir/Au contact were 3.7×10^{-8} A/cm^2 and 8.3×10^{-9} A/cm^2, respectively. Although the responsivities of these two different PDs are almost the same, the rejection ratio of AlInGaN MIS PD with a Ni/Ir/Au contact was larger than that of PD with a Ni/Au contact.

Acknowledgements

Funding from the Advanced Optoelectronic Technology Center, National Cheng Kung University, under projects from the Ministry of Education and the National Science Council of Taiwan (NSC 96-2221-E-006-079-MY3) are gratefully acknowledged. This work was also partially supported by the TDPA "Lamp Development of White Light-Emitting Diode for Local Lighting" program, the National Science Council of the Republic of China (ROC) in Taiwan under grants (TDPA 97-EC-17-A-07-S1-105 and NSC 97-2623-E-168-001-IT) and the Chung Shan Institute of Science and Technology.

References

[1] Nakamura S, Senoh M, Iwasa N, Nagahama SC. High-power InGaN single-quantum-well-structure blue and violet light-emitting diodes. Appl Phys Lett 1995;67:1868–70.
[2] Nakamura S, Senoh M, Nagahama S, Iwasa N, Yamada T, Matsushita T, et al. High-power Long-lifetime InGaN multi-quantum-well structure laser diodes. Jpn J Appl Phys 1997;36:L1059–61.
[3] Walker D, Monroy E, Kung P, Wu J, Hamilton M, Sanchez FJ, et al. High-speed, low-noise metal–semiconductor–metal ultraviolet photodetectors based on GaN. Appl Phys Lett 1999;74:762–4.
[4] Mazzeo G, Reverchon JL, Duboz JY, Dussaigne A. AlGaN-based linear array for UV solar-blind imaging from 240 to 280 nm. IEEE Sens J 2006;6:957–63.
[5] Saito W, Nitta T, Kakiuchi Y, Saito Y, Tsuda K, Omura I, et al. A 120-W boost converter operation using a high-voltage GaN-HEMT. IEEE Electron Dev Lett 2008;29:8–10.
[6] Hongtao X, Gao S, Heikman S, Long SI, Mishra UK, York RA. A high-efficiency class-E GaN HEMT power amplifier at 1.9 GHz. IEEE Microw Wirel Compon Lett 2006;16:22–4.
[7] Monroy E, Calle F, Pau JL, Sanchez FJ, Munoz E. Analysis and modeling of $Al_xGa_{1-x}N$-based Schottky barrier photodiodes. J Appl Phys 2000;88:2081–91.
[8] Liu SS, Li PW, Lan WH, Lin WJ. Improvements of AlGaN/GaN p–i–n UV sensors with graded AlGaN layer for the UV-B (280–320 nm) detection. Mater Sci Eng B 2005;122:196–200.
[9] Li T, Lambert DJH, Wong MM, Collins CJ, Yang B, Beck AL, et al. Low-noise back-illuminated $Al_xGa_{1-x}N$-based p–i–n solar-blind ultraviolet photodetectors. IEEE J Quantum Electron 2001;37:538–45.
[10] Wu MF, Yao S, Vantomme A, Hogg S, Langouche G, Van der Stricht W, et al. Elastic strain in InGaN and AlGaN layers. Mater Sci Eng B 2000;75:232–5.

[11] MONEMAR B. III–V nitrides: important future electronic materials. J Mater Sci 1999;10:227–54.
[12] Hirayama H, Akita K, Kyono T, Nakamura T, Ishibashi K. High-efficiency 352 nm quaternary InAlGaN-based ultraviolet light-emitting diodes grown on GaN substrates. Jpn J Appl Phys 2004;43(2):L1241–3.
[13] Mohammad SN, Fan Z, Botchkarev AE, Kim W, Aktas O, Salvador A, et al. Near-ideal platinum–GaN Schottky diodes. Electron Lett 1996;32:598–9.
[14] Miura N, Nanjo T, Suita M, Oishi T, Abe Y, Ozeki T, et al. Thermal annealing effects on Ni/Au based Schottky contacts on n-GaN and AlGaN/GaN with insertion of high work function metal. Solid-State Electron 2004;48:689–95.
[15] Readinger ED, Luther BP, Mohney SE, Piner EL. Environmental aging of Schottky contacts to n-AlGaN. J Appl Phys 2001;89:7983–7.
[16] Jeon CM, Jang HW, Lee JL. Thermally stable Ir Schottky contact on AlGaN/GaN heterostructure. Appl Phys Lett 2003;82:391–3.
[17] Kim JK, Jang HW, Jeon CM, Lee JL. GaN metal–semiconductor–metal ultraviolet photodetector with IrO_2 Schottky contact. Appl Phys Lett 2002;81:4655–7.
[18] Jang HW, Lee JL. Transparent ohmic contacts of oxidized Ru and Ir on p-type GaN. J Appl Phys 2003;93:5416–21.
[19] Aumer ME, LeBoeuf SF, McIntosh FG, Bedair SM. High optical quality AlInGaN by metalorganic chemical vapor deposition. Appl Phys Lett 1999;75:3315–7.
[20] Williams CK, Glisson TH, Hauser JR, Littlejohn MA. Energy bandgap and lattice constant contours of III–V quaternary alloys of the form $A_xB_yC_zD$ or $AB_xC_yD_z$. J Electron Mater 1978;7:639–46.
[21] Zhou JJ, Wen B, Jiang RL, Liu CX, Ji XL, Xie ZL, et al. Photoresponse of the $In_{0.3}Ga_{0.7}N$ metal insulator semiconductor photodetectors. Chin Phys 2007;16(7):2120–2.
[22] Sze SM. Semiconductor device physics and technology. Taiwan: John Wiley & Sons; 1983. p. 362.
[23] Jeon CM, Park KY, Lee JH, Lee JH, Lee JL. Thermally stable AlGaN/GaN heterostructure field-effect transistor with IrO_2 gate electrode. J Vac Sci Technol 2006;B24:1303–7.
[24] Lin ZJ, Lu W, Lee J, Liu DM, Flynn JS, Brandes GR. Barrier heights of Schottky contacts on strained AlGaN/GaN heterostructures: determination and effect of metal work functions. Appl Phys Lett 2003;82:4364–6.
[25] Zhong H, Heuss G, Misra V, Luan H, Lee CH, Kwong DL. Characterization of RuO_2 electrodes on ZrO_2. Appl Phys Lett 2001;78:1134–6.
[26] Han SY, Jang HW, Lee JL. IrO_2 Schottky contact on n-type 4H–SiC. Appl Phys Lett 2003;82:4726–8.
[27] Ishikawa T, Abe Y, Kawamura M, Sasaki K. Formation process and electrical property of IrO_2 thin films prepared by reactive sputtering. Jpn J Appl Phys 2003;42:213–6.
[28] Chen RS, Chang HM, Huang YS, Tsai DS, Chattopadhyay S, Chen KH. Growth and characterization of vertically aligned self-assembled IrO_2 nanotubes on oxide substrates. J Cryst Growth 2004;271:105–12.